Spectrochimica Acta Part A: Molecular and Biomolecular Spectroscopy 126 (2014) 164–169

Contents lists available at ScienceDirect

Spectrochimica Acta Part A: Molecular and Biomolecular Spectroscopy

journal homepage: www.elsevier.com/locate/saa

A Raman and infrared spectroscopic analysis of the phosphate mineral wardite $NaAl_3(PO_4)_2(OH)_4{\cdot}2(H_2O)$ from Brazil

Ray L. Frost [a,*], Ricardo Scholz [b], Andrés López [a], Cristiano Lana [b], Yunfei Xi [a]

[a] School of Chemistry, Physics and Mechanical Engineering, Science and Engineering Faculty, Queensland University of Technology, GPO Box 2434, Brisbane, Queensland 4001, Australia
[b] Geology Department, School of Mines, Federal University of Ouro Preto, Campus Morro do Cruzeiro, Ouro Preto, MG 35400-00, Brazil

HIGHLIGHTS

- A wardite mineral sample from Lavra Da Ilha, Minas Gerais, Brazil was analysed.
- Using SEM with EDX and vibrational spectroscopy.
- The calculated formula is $(Na_{0.97}Ca_{0.03})_{\Sigma 1.00}Al_3(PO_4)_2(OH)_4{\cdot}2(H_2O)$.
- Observation of multiple bands supports the concept of non-equivalent phosphate units in the structure.

GRAPHICAL ABSTRACT

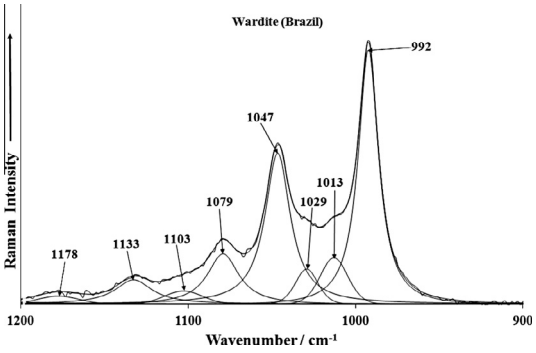

ARTICLE INFO

Article history:
Received 17 November 2013
Received in revised form 7 January 2014
Accepted 2 February 2014
Available online 15 February 2014

Keywords:
Wardite
Cyrilovite
Phosphate
Hydroxyl
Raman spectroscopy

ABSTRACT

A wardite mineral sample from Lavra Da Ilha, Minas Gerais, Brazil has been examined by vibrational spectroscopy. The mineral is unusual in that it belongs to a unique symmetry class, namely the tetragonal-trapezohedral group. The structure of wardite contains layers of corner-linked –OH bridged MO_6 octahedra stacked along the tetragonal *C*-axis in a four-layer sequence and linked by PO_4 groups. Consequentially not all phosphate units are identical. Two intense Raman bands observed at 995 and 1051 cm^{-1} are assigned to the ν_1 PO_4^{3-} symmetric stretching mode. Intense Raman bands are observed at 605 and 618 cm^{-1} with shoulders at 578 and 589 cm^{-1} are assigned to the ν_4 out of plane bending modes of the PO_4^{3-}. The observation of multiple bands supports the concept of non-equivalent phosphate units in the structure. Sharp infrared bands are observed at 3544 and 3611 cm^{-1} are attributed to the OH stretching vibrations of the hydroxyl units. Vibrational spectroscopy enables subtle details of the molecular structure of wardite to be determined.

Introduction

Wardite is a mineral found in many parts of the world, including Brazil. Wardite [1] is a hydrated hydroxyl sodium aluminium phosphate $NaAl_3(PO_4)_2(OH)_4{\cdot}2(H_2O)$ [2,3]. Wardite is a poorly known mineral, but of special interest to mineralogists. Some studies of wardite and the structurally related mineral cyrilovite have been undertaken by the authors [4,5]. Hence, we have carried out this study to further our understanding of the structure of the mineral wardite. Crystals of wardite show the lower symmetry by displaying squashed psuedo-octahedrons with striated faces. The mineral is unusual in that it belongs to a unique symmetry class, namely the tetragonal-trapezohedral group [2]. This class has only a 4-fold rotational axis and two 2-fold rotational axes and nothing else. Such

* Corresponding author. Tel.: +61 7 3138 2407; fax: +61 7 3138 1804.
E-mail address: r.frost@qut.edu.au (R.L. Frost).

http://dx.doi.org/10.1016/j.saa.2014.02.007
1386-1425/

unique symmetry will influence the vibrational spectrum. Crystals of wardite show the lower symmetry by displaying squashed psuedo-octahedrons with striated faces. The crystal structures of natural wardite and of the isomorphous cyrilovite are published [2,6]. The structure of cyrilovite was further refined by Cooper et al. [7]. The cell dimensions are *Space Group:* $P4_12_12$ or $P4_32_12$. $a = 7.03(1)$ Å, $c = 19.04(1)$ Å and $Z = 4$. The structures contain layers of two kinds of corner-linked –OH bridged MO_6 octahedra (M = Al, Fe), stacked along the tetragonal *C*-axis in a four-layer sequence and linked by PO_4 groups. Within a layer, e.g. around the (0 0 1) plane, two independent pairs of symmetry-correlated –OH groups are arranged in the equatorial pseudo-planes of one kind of MO_6 octahedra [2,6]. The mineral is white to colourless, to pale green to blue–green and other colours depending upon the composition of the mineral. Wardite is an Al based mineral but replacement of the Al by Fe will affect the exact colour of wardite. The mineral is known from many localities in Australia including at the Iron Monarch quarry, Iron Knob, South Australia, from Wycheproof, Victoria, and on Milgun Station, Western Australia.

There have been some studies of the vibrational spectroscopy of wardite [8,9]. Tarte et al. collected the infrared spectra of five samples of cyrilovite $NaFe_3(PO_4)_2(OH)_4{\cdot}2(H_2O)$ and wardite [9]. Cyrilovite is analogous to wardite, with ferric iron replacing the aluminium in the structure. It is likely that solid solutions of the two minerals are formed with varying amounts of ferric ion and aluminium in the structure, thus influencing the colour and appearance of the mineral. The mineral wardite is capable of crystallizing in a similar form to that of cyrilovite because of their closely related chemical compositions. Between wardite's composition, $NaAl_3(PO_4)_2(OH)_4{\cdot}2(H_2O)$, and cyrilovite composition, $NaFe_3(PO_4)_2(OH)_4{\cdot}2(H_2O)$, these minerals are able to form end members of a series of solid solutions. Either of the two minerals can occur in various proportions in a series of solid solutions in the wardite mineral group. Cyrilovite is a rare accessory mineral in some oxidizing phosphate-bearing granite pegmatites and iron deposits, such as are found in Brazil [4].The vibrational spectrum is dependent upon the ratio of the Al/Fe. Tarte et al. found that the two minerals wardite and cyrilovite can be distinguished by the spectral patterns of the OH stretching region in the infrared spectrum [9]. These workers did not interpret the spectra of the phosphate because of complexity and no detailed assignment was given. Breitinger et al. reported the combined vibrational spectra of a natural wardite. Breitinger and co-workers used a full array of techniques including inelastic neutron scattering, infrared, Raman and near infrared techniques [8] to study the properties of the mineral. These workers used a natural wardite with significant amounts of ferric iron in the structure. In other words the sample analysed was fundamentally a solid solution of wardite and cyrilovite, but at the wardite end. The original papers on the infrared spectrum of isolated phosphate units was published by Lazarev [10]. Of course, Phosphates structures are different. Usually they have rather low symmetry: orthorhombic, monoclinic, or even triclinic [11]. Farmer based upon the work of Petrov et al. [12–14] made a comparison of the results of the vibrational spectrum of a series of phosphates.

Raman spectroscopy has proven very useful for the study of minerals, especially minerals containing oxyanions such as phosphate. Indeed, Raman spectroscopy has proven most useful for the study of diagenetically related minerals where isomorphic substitution may occur as with wardite and cyrilovite, as often occurs with minerals containing phosphate groups. This paper is a part of systematic studies of vibrational spectra of minerals of secondary origin in the oxide supergene zone. The objective of this research is to report the Raman and infrared spectra of wardite and to relate the spectra to the molecular structure of the mineral.

Experimental

Samples description and preparation

The mineral wardite studied in this work was obtained from the collection of the Geology Department of the Federal University of Ouro Preto, Minas Gerais, Brazil, with sample code SAD-008. The wardite originated from Lavra Da Ilha, Minas Gerais, Brazil. Details of the mineral have been published (page 643) [15]. Crystals of wardite can make nice specimens with their colourless or light green colour and glassy lustre. Massive green wardite is associated with variscite nodules where it formed from the alteration of the variscite. The mineral is an uncommon species in complex zoned pegmatites.

The sample was gently crushed and the associated minerals were removed under a stereomicroscope Leica MZ4. Scanning electron microscopy (SEM) was applied to support the mineral chemistry.

Scanning electron microscopy (SEM)

Wardite cleavage fragments were coated with a 5 nm layer of evaporated Au. Secondary Electron and Backscattering Electron images were obtained using a JEOL JSM-6360LV equipment. Qualitative and semi-quantitative chemical analyses in the EDS mode were performed with a ThermoNORAN spectrometer model Quest and were applied to support the mineral characterization.

Raman spectroscopy

Crystals of wardite were placed on a polished metal surface on the stage of an Olympus BHSM microscope, which is equipped with 10×, 20×, and 50× objectives. The microscope is part of a Renishaw 1000 Raman microscope system, which also includes a monochromator, a filter system and a CCD detector (1024 pixels). The Raman spectra were excited by a Spectra-Physics model 127 He–Ne laser producing highly polarised light at 633 nm and collected at a nominal resolution of 2 cm^{-1} and a precision of ±1 cm^{-1} in the range between 200 and 4000 cm^{-1}. Some of these mineral fluoresced badly at 633 nm; as a consequence other laser excitation wavelengths were used especially the 785 nm laser. Repeated acquisitions on the crystals using the highest magnification (50×) were accumulated to improve the signal to noise ratio of the spectra. Spectra were calibrated using the 520.5 cm^{-1} line of a silicon wafer. Previous studies by the authors provide more details of the experimental technique [4,16–19]. Alignment of all crystals in a similar orientation has been attempted and achieved. However, differences in intensity may be observed due to minor differences in the crystal orientation.

Infrared spectroscopy

Infrared spectra were obtained in reflectance mode, using a Nicolet Nexus 870 FTIR spectrometer with a smart endurance single bounce diamond ATR cell. Spectra over the 4000–525 cm^{-1} range were obtained by the co-addition of 128 scans with a resolution of 4 cm^{-1} and a mirror velocity of 0.6329 cm/s. Spectra were co-added to improve the signal to noise ratio. Using the reflectance technique, the mineral sample is not destroyed. This is important as many mineral samples are from museum collections, as is this sample.

Spectral manipulation such as baseline correction/adjustment and smoothing were performed using the Spectracalc software package GRAMS (Galactic Industries Corporation, NH, USA). Band component analysis was undertaken using the Jandel 'Peakfit'

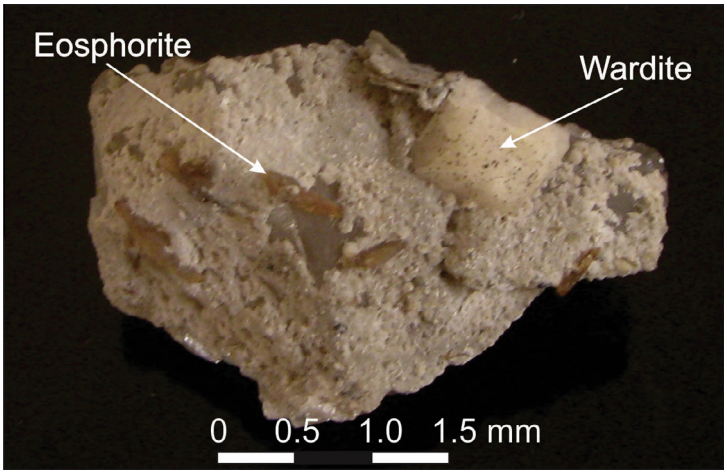

Fig. 1. SEM image of Brazilian wardite.

software package that enabled the type of fitting function to be selected and allows specific parameters to be fixed or varied accordingly. Band fitting was done using a Lorentzian–Gaussian cross-product function with the minimum number of component bands used for the fitting process. The Gaussian–Lorentzian ratio was maintained at values greater than 0.7 and fitting was undertaken until reproducible results were obtained with squared correlations of r^2 greater than 0.995.

Results and discussion

Chemical characterization

The BSI image of wardite sample studied in this work is shown in Fig. 1. Qualitative and semi-quantitative chemical composition shows a Na and Al phosphate phase. Minor amount of Ca is also observed. The chemical analysis is represented as an EDS spectrum in Fig. 2. On the basis of semiquantitative chemical analyses the chemical formula was calculated an can be expressed as $(Na_{0.97}Ca_{0.03})_{\Sigma 1.00}Al_3(PO_4)_2(OH)_4{\cdot}2(H_2O)$.

Vibrational spectroscopy

The Raman spectrum of wardite over the 100–4000 cm^{-1} spectral range is reported in Fig. 3a. The spectrum shows complexity

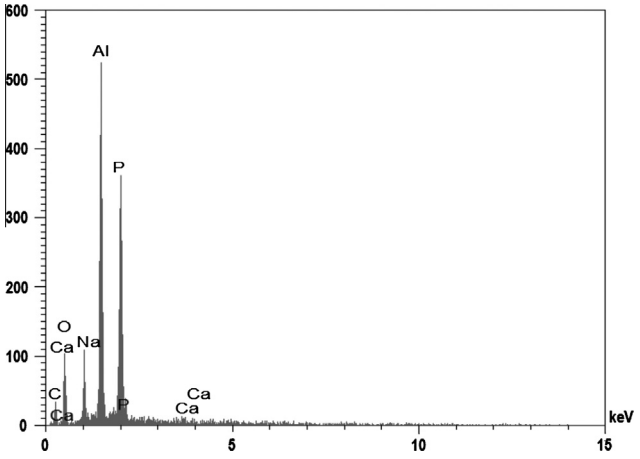

Fig. 2. EDX analysis of Brazilian wardite.

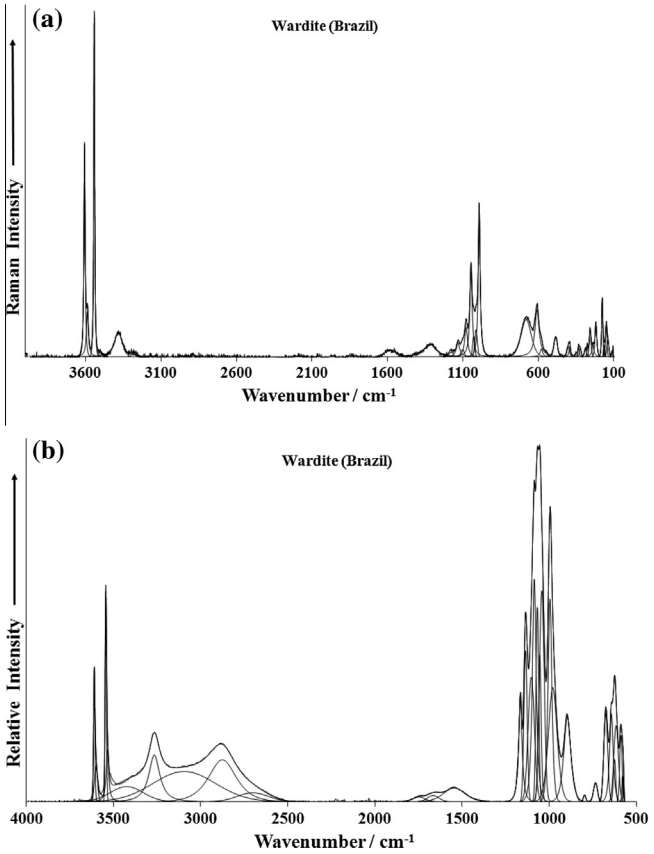

Fig. 3. (a) Raman spectrum of wardite over the 100–4000 cm^{-1} spectral range. (b) Infrared spectra of wardite over the 500–4000 cm^{-1} spectral range.

with many bands being observed. Such complexity reflects the loss of symmetry of the phosphate anion. This figure of the Raman spectrum shows the position and relative intensities of the Raman bands. It is noteworthy that there are large parts of the spectrum where no intensity is observed. The Raman spectrum is therefore, subdivided into sections depending upon the type of vibration being analysed. The infrared spectrum of wardite over the 500–4000 cm^{-1} spectral range is displayed in Fig. 3b. The spectrum is not shown below 500 cm^{-1}. The reason for this is that we are using a reflectance technique and the ATR cell absorbs all incident

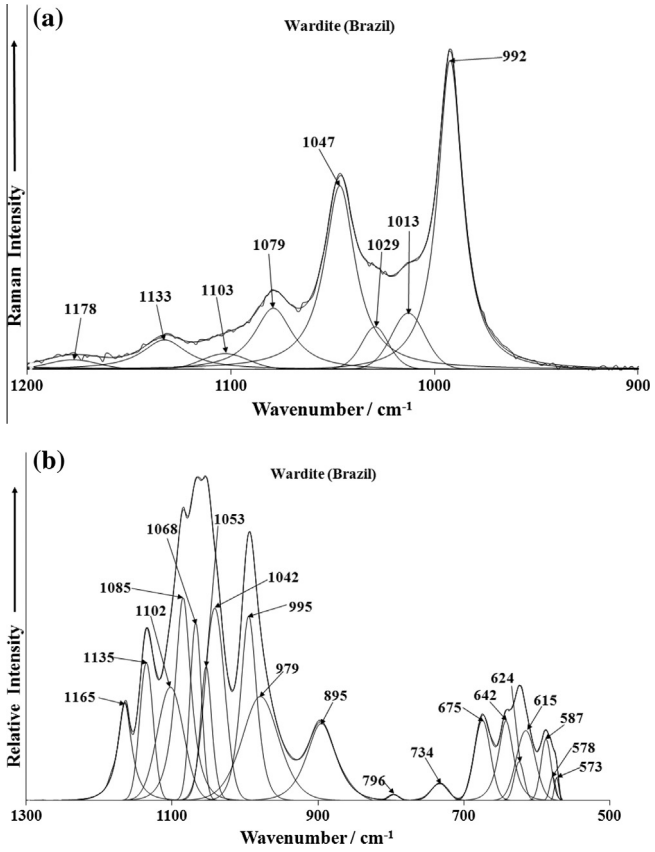

Fig. 4. (a) Raman spectrum of wardite over the 800–1400 cm^{-1} range. (b) Infrared spectrum of wardite over the 500–1300 cm^{-1} range.

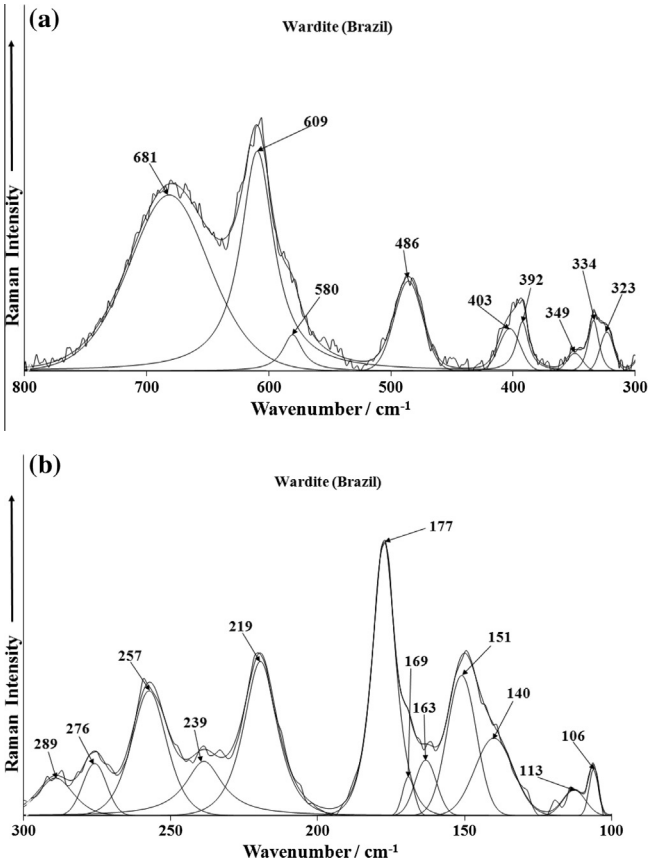

Fig. 5. (a) Raman spectrum of wardite over the 300–800 cm^{-1} range. (b) Raman spectrum of wardite over the 100–300 cm^{-1} range.

radiation. There are parts of this infrared spectrum where little or no intensity is observed. This spectrum may be thus subdivided into sections depending upon the type of vibration being analysed.

The Raman spectrum of wardite from Brazil in the 800–1300 cm^{-1} region is displayed in Fig. 4a. However, the spectrum appears to differ considerably from that obtained by Breitinger et al. In the work of Breitinger et al., these authors did not study naturally occurring minerals but rather used synthetic analogs of the wardite mineral. The spectra are dominated by two intense bands at around 995 and 1051 cm^{-1}. These two bands are assigned to the ν_1 PO_4^{3-} symmetric stretching vibrations. Two intense Raman bands are observed reflecting two non-equivalent phosphate units in the wardite structure. Breitinger et al. used FT-Raman to obtain their spectra and found overlapping Raman bands at 999 and 1033 cm^{-1} and assigned these bands to the ν_1 PO_4^{3-} symmetric stretching and ν_3 PO_4^{3-} antisymmetric stretching modes. The difference in the spectra between our work and that of Breitinger et al. may be attributed to the improved technology of the spectrometer with greater resolution.

Breitinger et al. also assigned the band at 999 cm^{-1} to AlOH deformation modes. In this work the band at 995 cm^{-1} is very sharp and well resolved. The band at 1051 cm^{-1} is ever so slightly asymmetric on the low wavenumber side and a component may be resolved at 1045 cm^{-1}. A group of low intensity bands are observed at 1083, 1109, 1140 and 1186 cm^{-1} and are assigned to the ν_3 PO_4^{3-} antisymmetric stretching modes. Breitinger et al. did not report any bands in these positions in the Raman spectrum. These workers reported infrared bands at 1058 (strong) with shoulders at 1129 and 1168 cm^{-1} and assigned these bands to δAl_2OH deformation modes. A low intensity broad band at 884 cm^{-1} (a), 902 cm^{-1} (b) and 893 cm^{-1} (c) are assigned to a water librational modes. In the work of Breitinger et al. a broad low intensity band was found at around 800 cm^{-1} and was attributed to water librational modes.

The infrared spectrum of wardite from Brazil is displayed in Fig. 4b. The infrared spectra show a great deal more complexity than the Raman spectra. This no doubt results from the difference in spatial resolution. The spatial resolution of the Raman spectrometer is around 1 μm, as compared with the infrared spectrometer where the spatial resolution of around 30 μm is used. The band at around 994 cm^{-1} is attributed to the ν_1 PO_4^{3-} symmetric stretching mode. The cluster of bands at 1042, 1053, 1085, 1102, 1135 and 1165 cm^{-1} are attributed to the ν_3 PO_4^{3-} antisymmetric stretching modes. Some of these bands may also be due to the δAl_2OH deformation modes, in harmony with the assignment of Breitinger et al. He and his co-workers stated that the deceptively simple strong IR band centered at 1059 cm^{-1} contains at least four components of $\nu(PO_4)$ generated by lifting of the originally threefold degeneracy of $\nu_3(PO_4)$ and activation of $\nu_1(PO_4)$ due to the general position of PO_4 and again at least four components of the deformation modes $\delta(Al_2OH)$ involving the two pairs of the non-equivalent OH groups. In this work we have obtained much greater resolution and these bands are resolved into the component bands.

The Raman spectral region of the phosphate bending modes is reported in Fig. 5a. Intense Raman bands are observed at 588 and 620 with an additional band at 559 cm^{-1} are assigned to the ν_4 out of plane bending modes of the PO_4^{3-} and $HOPO_3^{2-}$ units. Breitinger et al. assigned these bands to $\nu(Al(O/OH)_6)$ stretching vibrations. No phosphate bending modes in the work of Breitinger et al. were reported. However, such bands must be present in the spectra. The Raman spectrum of crystalline NaH_2PO_4 shows Raman bands at 526, 546 and 618 cm^{-1} (data obtained by the authors). A series of bands are observed at 396, 416, 444, 464, and 489 cm^{-1}. These bands are attributed to the ν_2 PO_4^{3-} and H_2PO_4 bending modes. The Raman spectrum of NaH_2PO_4 shows Raman bands at 460 and 482 cm^{-1}. Thus, the series of Raman bands at 391, 401,

458, 485 and 510 cm^{-1} is attributed to the ν_2 PO_4^{3-} bending modes. Raman bands at 317, 446 and 515 cm^{-1} reported by Breitinger et al. were assigned to vibrational modes of the AlO_6/$AlOH_6$ units.

In the infrared spectrum (Fig. 4b) a series of bands are observed at 620, 643 and 673 cm^{-1}. These bands are attributed to the ν_4 out of plane bending modes of the PO_4^{3-} units. Breitinger et al. assigned bands in this region to $\nu(Al(O/OH)_6)$ stretching vibrations. In harmony with Breitinger et al. assignments, the infrared bands observed at 732, 795 and 893 cm^{-1} are attributed to water librational modes. Infrared bands for the wardite mineral sample from Brazil are observed at 573, 578 and 587 cm^{-1}. These bands are attributed to $\gamma(Al_2OH)$ vibrations. The Raman spectrum of wardite in the 100–300 cm^{-1} region is shown in Fig. 5b. Intense Raman bands observed at 299 cm^{-1} for the Brazilian wardite are related to the O–Al–O skeletal stretching vibrations. The intense band in all the spectra at 177 cm^{-1} is considered to be due to H–OH hydrogen bonds.

The Raman spectrum of the wardite mineral sample from Brazil is reported in Fig. 6a. Intense Raman bands are observed at 3536, 3545 and 3611 cm^{-1} and are assigned to the stretching vibration of the hydroxyl units. The broad Raman bands at 2876, 3266, 3425 cm^{-1} is attributed to water stretching vibrations. Sharp infrared bands are observed at 3545 and 3611 cm^{-1} are attributed to the OH stretching vibrations of the hydroxyl units. Two shoulder bands are observed at 3532 and 3601 cm^{-1} are also assigned to the OH stretching vibrations. Breitinger et al. [8] found infrared bands at 3520 (vw), 3545 (s), 3585 (sh) and 3613 cm^{-1} (m). Breitinger et al. states that the ν(OH) modes in the two independent pairs of symmetry-correlated OH groups classify as $2a + 2b$; with the correlation splitting between a and b species depending on the distances in each of the pairs [8]. The ν(OH) region of IR spectra

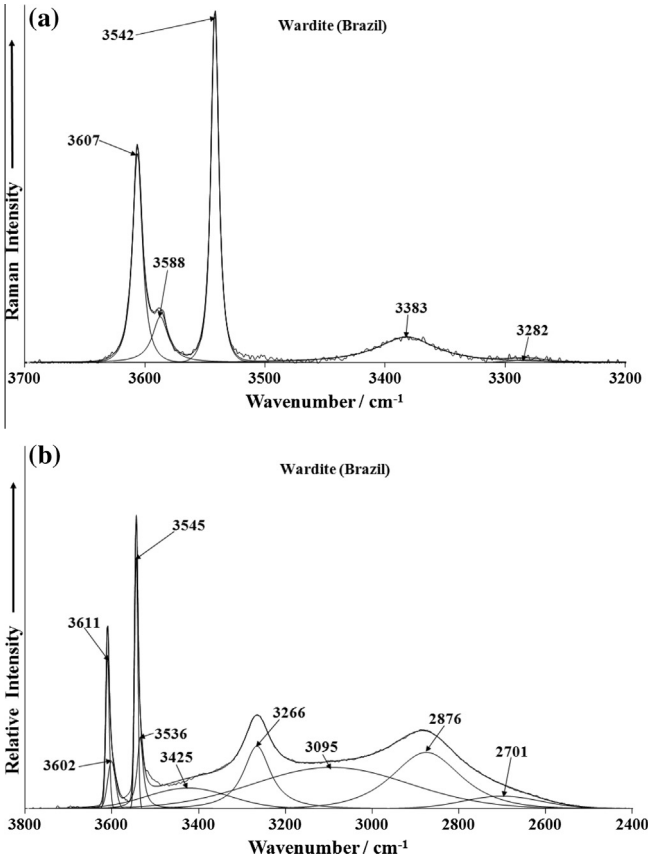

Fig. 6. (a) Raman spectrum of wardite over the 2600–3800 cm^{-1} spectral range. (b) Infrared spectrum of wardite over the 2400–3800 cm^{-1} range.

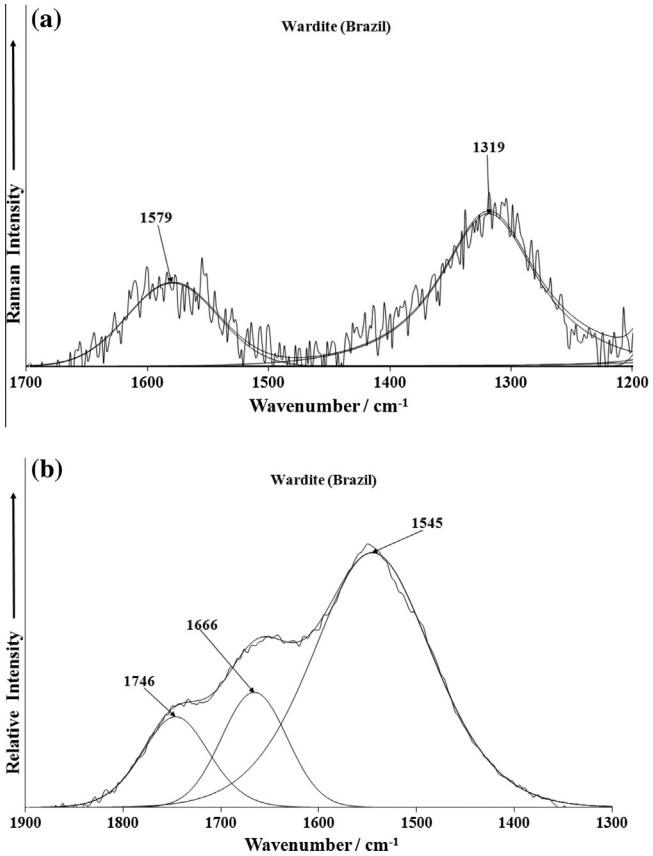

Fig. 7. (a) Raman spectrum of wardite over the 1400–1800 cm^{-1} spectral range. (b) Infrared spectrum of wardite over the 1300–1900 cm^{-1} range.

of wardite shows two sharp bands (3613 and 3545 cm^{-1}) with two weak shoulders or satellites (3580 and 3520 cm^{-1}). It is likely that the two sharp infrared bands are due to two independent and non-equivalent OH units. The two sharp shoulder bands may be attributed to the Al–OH–Fe groups, i.e. the cyrilovite part of the solid solution.

Broad infrared bands are observed at 2876 and 3266 cm^{-1}. These bands are assigned to water stretching vibrations. It is probable that some of the component bands are due to overtones and combination of the water bending and librational modes. The position of the water stretching vibration provides evidence for strong hydrogen bonding and that water is involved in different hydrogen bonding arrangements. The band at around 2876 cm^{-1} gives an indication that water is very strongly hydrogen bonded in the wardite structure. The Raman spectrum of the wardite from Brazil in the 1200–1700 cm^{-1} spectral range is illustrated in Fig. 7a. Two Raman bands are found at 1319 and 1579 cm^{-1}. The infrared spectrum of the wardite mineral sample from Brazil over the 1300–1900 cm^{-1} spectral range is shown in Fig. 7b. Infrared bands are observed at 1545, 1666 and 1746 cm^{-1}. The bands in this region result from correlation splitting as a result of the short distance and orientation of the H_2O molecules.

Conclusions

Raman spectroscopy complimented with infrared spectroscopy has been used to study the molecular structure of mineral wardite from Brazil. The structure of wardite is unusual in that it belongs to a unique symmetry class, namely the tetragonal-trapezohedral group. The structure of wardite contains layers of corner-linked –OH bridged MO_6 octahedra stacked along the tetragonal C-axis in a

four-layer sequence and linked by PO_4 groups. As a consequence at the molecular level non-equivalent phosphate units exist in the structure. As a consequence multiple phosphate vibrational modes are observed. Vibrational spectroscopy offers new information on the structure of naturally occurring wardite.

Acknowledgments

The financial and infra-structure support of the Discipline of Nanotechnology and Molecular Science, Science and Engineering Faculty of the Queensland University of Technology, is gratefully acknowledged. The Australian Research Council (ARC) is thanked for funding the instrumentation. The authors would like to acknowledge the Center of Microscopy at the Universidade Federal de Minas Gerais (http://www.microscopia.ufmg.br) for providing the equipment and technical support for experiments involving electron microscopy. R. Scholz thanks to CNPq – Conselho Nacional de Desenvolvimento Científico e Tecnológico (Grants Nos. 306287/2012-9 and 402852/2012-5).

Appendix A. Supplementary material

Supplementary data associated with this article can be found, in the online version, at http://dx.doi.org/10.1016/j.saa.2014.02.007.

References

[1] J.M. Davison, Am. J. Sci. 2 (1896) 154–155.
[2] L. Fanfani, A. Nunzi, P.F. Zanazzi, Min. Mag. 37 (1970) 598–605.
[3] M.L. Lindberg, Am. Mineral. 42 (1957) 204–213.
[4] R.L. Frost, Y. Xi, R. Scholz, Spectrochim. Acta A 108 (2013) 244–250.
[5] R.L. Frost, Y. Xi, Spectrochim. Acta A 93 (2012) 155–163.
[6] D. Cozzupoli, O. Grubessi, A. Mottana, P.F. Zanazzi, Mineral. Petrol. 37 (1987) 1–14.
[7] M.A. Cooper, F.C. Hawthorne, P. Cerny, J. Czech Geol. Soc. 45 (2000) 95–100.
[8] D.K. Breitinger, H.H. Belz, L. Hajba, V. Komlosi, J. Mink, G. Brehm, D. Colognesi, S.F. Parker, R.G. Schwab, J. Mol. Struct. 706 (2004) 95–99.
[9] P. Tarte, A.M. Fransolet, F. Pillard, Bull. Min. 107 (1984) 745–754.
[10] A.N. Lazarev, Nauka (1968).
[11] W. Jastrzebski, M. Sitarz, M. Rokita, K. Bulat, Spectrochim. Acta A 79 (2011) 722–727.
[12] I. Petrov, B. Soptrajanov, N. Fuson, Zeit. Anorgan. Allgemeine Chem. 358 (1968) 178–186.
[13] I. Petrov, B. Soptrajanov, N. Fuson, J.R. Lawson, Spectrochim. Acta A 23 (1967) 2637–2646.
[14] K.I. Petrov, I.V. Tananaev, V.G. Pervykh, S.M. Petushkova, Zh. Neorgan, Zh. Neorgan. Khim. 12 (1967) 2645–2650.
[15] J.W. Anthony, R.A. Bideaux, K.W. Bladh, M.C. Nichols, Handbook of Mineralogy, Mineral Data Publishing, Tuscon, Arizona, USA, 1995.
[16] R.L. Frost, S.J. Palmer, Y. Xi, J. Cejka, J. Sejkora, J. Plasil, Spectrochim. Acta A 103 (2013) 431–434.
[17] R.L. Frost, Y. Xi, R. Scholz, M. Belotti Fernanda, A. Dias Menezes Filho Luiz, Spectrochim. Acta A 104 (2013) 250–256.
[18] R.L. Frost, A. Lopez, Y. Xi, A. Granja, R. Scholz, R.M.F. Lima, Spectrochim. Acta A 114 (2013) 309–315.
[19] R.L. Frost, Y. Xi, M. Beganovic, F.M. Belotti, R. Scholz, Spectrochim. Acta A 107 (2013) 241–247.